G. EJECTA DISTRIBUTION MODEL, SOUTH RAY CRATER

By GEORGE E. ULRICH, HENRY J. MOORE,
V. STEPHEN REED, EDWARD W. WOLFE, and KATHLEEN B. LARSON

CONTENTS

ILLUSTRATIONS

TABLES

INTRODUCTION

South Ray is a fresh, blocky crater, 680 m across and 135 m deep, in the southern part of the Apollo 16 landing site. Its bright rays extend northward radially across the traverse area. Sampling of ejects from South Ray was a prime objective of the mission because of its location on the Cayley plains, 6.2 km south of the Lunar Module (LM). Direct sampling and photographing of its rim and flanks, where less equivocal provenances could have been established, were prohibited by the distance from the LM, the limited time available for traversing, and the anticipated roughness of the terrain. Therefore additional evidence and interpretation are required to relate certain samples collected to South Ray.

The approach taken here in determining which of the localities sampled lie within rays of ejects from South Ray crater and to what extent or depth these localities may have been covered by ejects is to estimate the apparent volume of the crater and then to distribute this volume as ejects using several models. In one set of models, ejects are confined within observable ray patterns; in a second set, ejects are not confined. The purpose of this chapter is to determine a reasonable model for the areal distribution and variation in thickness of ejects material within rays as a function of distance from South Ray crater. A stratigraphic interpretation of materials ejected from South Ray is treated elsewhere (AFGIT, 1973; Ulrich and Reed, this volume).

DEFINITION OF SOUTH RAY EJECTA

Part of the problem in defining South Ray ejects is to

establish those properties that characterize the ejecta on the lunar surface and correlate them with reflected brightness and topography using the best available orbital photography. Block concentrations, surfaces disturbed by the impact of ballistic debris, lineations produced by deposition of ejecta, and individual secondary craters were observed on a local scale by the astronauts and can be seen in photographs taken by them. For a crater the size of South Ray, these features, are not resolvable on orbital photographs except at a few places. The properties of crater ejecta seen on orbital photography are reflected brightness and irregularities in topographic expression. Bright areas around young lunar craters photographed under high sun-elevation angles are produced by a combination of effects: (1) concentrations of blocks and rock fragments, (2) steep surface slopes, and (3) composition of material. Brightness contrasts in surface materials of a crater and its ejecta decrease with the age of the crater. Topographic expression of ejecta is most evident near the crater, and its definition is a function of photographic resolution. For South Ray, contrasts in reflected brightness were to delineate the ejecta on orbital photography, because the high sun-elevation angle of available photographs proved to be a sensitive indicator of ejecta distribution (figs. 1 and 2). The distribution of bright regions, including South Ray, its flanks, and rays or filaments extending radially from it, attest to the crater's youth. Bright areas beyond the rim are inferred to be covered partly to completely by ejecta from the crater.

MAPPING TECHNIQUES

Previous mapping of ejecta distribution around South Ray consisted of compilation by visual inspection Apollo 14 photographs (Hodges, 1972a; Elston others, 1972b; Muehlberger and others, 1972; fig. 1, pl.2 this volume). Here, digital processing of Apollo panoramic camera photographs taken when the sun-elevation angle was 60° was used to delineate the distribution of ejecta from South Ray beyond the crater flanks. An unaltered photograph of the landing site, figure 2, was digitized and, by means of computer filtering techniques, regenerated to enhance reflected brightness variations at three different levels (fig. 3). These images, together with figure 1 and selected premission photographs, were the basis for compilation of a ray map of South Ray ejecta (see Reed, fig. 4, this volume). The procedure required a minimum of arbitrary judgment in drawing the boundaries of ray-covered areas. The units mapped were designated as continuous thin to discontinuous, and discontinuous ejecta.

A topographic map of South Ray crater (fig. 4) enables us to estimate the amount of material ejected from South Ray, the height of the rim (fig. 5), and the thick ness of ejecta at the rim.

MEASUREMENT OF EJECTA- AND RAY-COVERED AREAS

The area covered by mappable rays was measured (at a scale of 1:50,000) with a planimeter, in concentric annuli (or bands) one crater diameter (680 m) wide, expanding outward from the crater rim, as illustrated by figure 6. A plot of the area of ejecta measured within each annulus, figure 7, shows the ejecta-covered areas to be clearly asymmetric in their distribution around South Ray. In each of the third through seventh annuli, however, they remain nearly constant at 7-9 km^2 while the total annulus area increases by 2.0 km^2 per ring. Beyond the seventh annulus, the ray-covered areas decrease at a nearly constant rate of 0.9 to 1.0 km^2 per annulus. Another means of viewing these data is to plot the percentage of total area within each annulus covered by ray material as a function of distance from South Ray rim (fig. 8). The histogram shows that only the six inner annuli are more than 50 percent covered and that all of the Apollo 16 samples come from annuli where less than 57 percent of the area is covered by mappable rays.

MEASUREMENT OF RIM HEIGHT AND CRATER VOLUME

Using the topographic map of South Ray (fig. 4), a precrater surface was estimated by extrapolating contours from outside the hummocky rim across the existing crater. Intersections of this surface with the crater wall determine the elevation of the original ground surface. Differences in elevation of points on the rim crest and the projected original ground surface beneath the points represent the rim height. Values obtained in this way range between 19 and 26 m; the average is 22 m. Another method of calculating these values is to determine the average difference in elevation between the rim crest and the outer margin of hummocky ejecta, shown in the sketch map (fig. 5) along with elevation differences between the rim crest and this edge. The range in values for rim height by this method is 13 to 28 m, the average about 20 m. From this, we consider the average rim height to be near 20-22 m.

The rim height includes two components, the amount that the original ground surface was uplifted and the thickness of the ejecta deposited on the uplifted surface (fig. 9). For terrestrial explosive craters, the percentage of the total rim height resulting from upwarping of ground surface ranges from 17 to 71 percent (Carlson and Jones, 1965, table 1); for six craters in alluvium 31 to 366 m across, an average of 45 percent of the rim height is the result of upwarp of the original ground surface. Recent drilling at Meteor Crater, Ariz., reveals that 35 to 60 percent of the present

FIGURE 1.- Premission photomosaic map of Apollo 16 landing site (Apollo 1470mm photographs 9515, 9520, 9522, 9530, and 9605, Mosaicking and rectification by G. M. Nakata, aiir brush retouching by P.M. Bridges, USGS Planetary Cartography Group, Flagstaff, Ariz.)

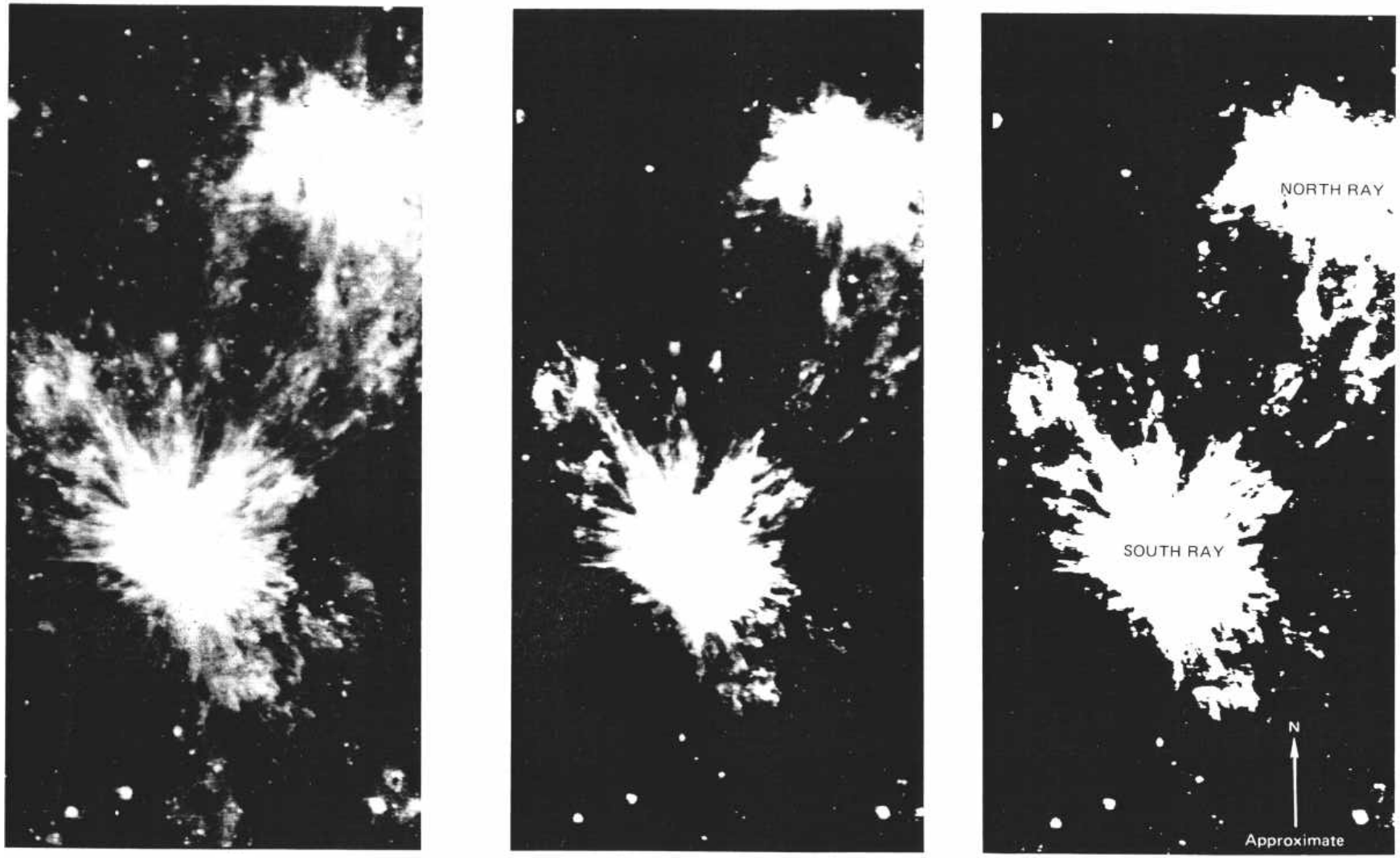

FIGURE 3. – Digitally enhanced regenerations of photograph in figure 2. *A*, *B*, and *C* are light, medium, and heavy "stretches" (high-pass filtered), respectively. Prepared by Anthony Hall, USGS Image Processing Facility, Flagstaff, Ariz.

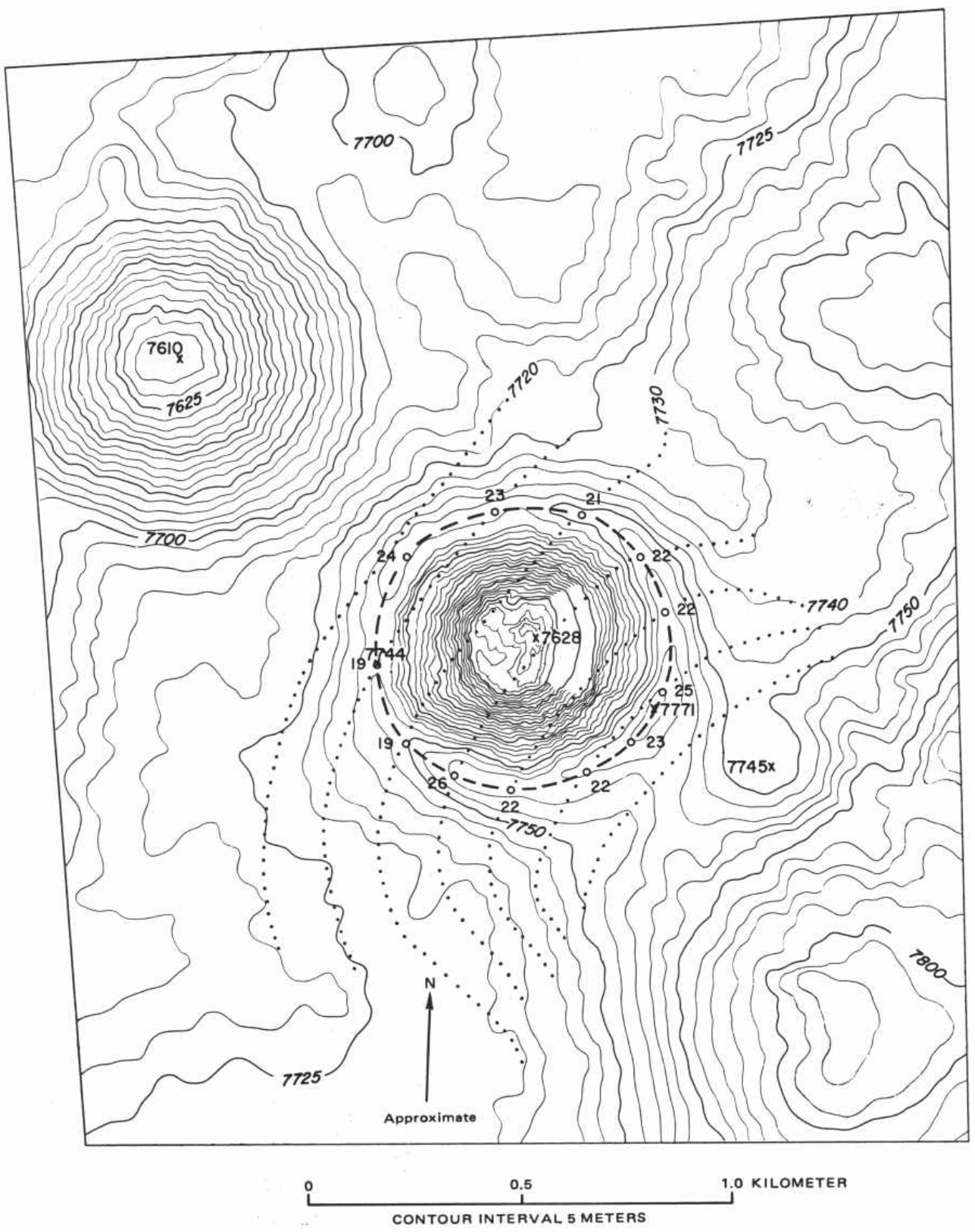

FIGURE 4.-Topographic map of South Ray crater. Dotted lines are extrapolated, contours of pre-South Ray surface. Dashed line shows crater rim crest; numbers are elevations (in meters) of the rim crest above the extrapolated original ground surface. Compilation scale 1:10,000; photographic model from Apollo 16 panoramic camera frames 4618 and 4623. Topography compiled by G. M. Nakata.

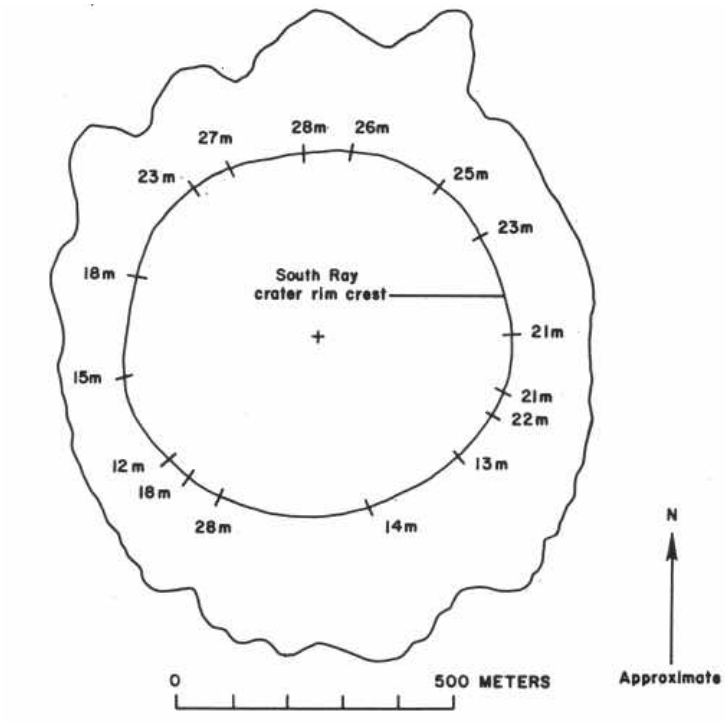

FIGURE 5.-Outline of hummocky ejects around South Ray crater rim (from J. P. Schafer, unpub. data,. 1973.) Values for height of rim were measured from figure 4 as the difference in elevation between edge of hummocky ejects and rim crest. Rim-crest diameter averages 680 m.

and others, 1972, fig. 6-6 and table-6-I). (4) By comparison with South Ray, the fragment population of the continuous ejects of North Ray crater generally occupies less than one percent of the area except on the rim crest, because erosional history is longer and the majority of North Ray rocks are more friable.

Some large concentrations of blocks are unrelated to North or South Ray. The highest block density found anywhere at the site was in an area about 700 m south of the LM (fig. 10*C*), where blocks occupy nearly 16 percent of the surface and probably represent the rim of afresh young crater 40 m in diameter. This area lies near a small bright ray radial to South Ray crater, where the block density is much higher than expected for South Ray material at this range (5.6 km). Farther from South Ray, mappable rays become thin and are difficult to recognize (fig. 10*D*).

DISTRIBUTION MODELS

With the quantitative estimates derived herein, we now combine the, orbital and surface information to construct models of ejects distribution. for South Ray crater. Having measured the volume of the apparent crater, 10 million m^3, its-rim height, 20-22 m, the area within which most of this ejects .was deposited, and the thickness of ejects at the crater rim, 10 -12 m, we can derive expressions that describe the distribution and thickness of ejects as a function of distance from the crater rim: The additional data of fragment counts per unit area made from photographs on the lunar surface permits a comparison of the volume of fragments larger than 2 cm in diameter with the ejects thicknesses predicted by various curves[1].

Carlson and Roberts (1963) have shown that the thickness of ejecta (*t*) as a function of distance from the center of the crater (*r*) can be approximately described by

$$t = K(r)S, \qquad (1)$$

where *K* is a constant and s is an exponent having values commonly near -2.0 to -3.5 The volume, *V*, of ejects deposited from the crater rim to infinity is given by

$$V = 2\pi K \frac{R^{S+2}}{s+2}$$

where *R* is the radius of the crater and s is less than minus 2: *R* for South Ray is 340 m. When *s* is exactly -2, another formula applies:

For our purposes, we will consider two. general models: (1) All ejects is confined to the mappable rays (Reed, fig. 4; this volume) and deposited within 16 crater diameters (*r*=11,220 m). (2) Ejecta is uniformly deposited from the rim outward to infinity with thickness decreasing according to equation (1). To test these models, we chose several values of *s*: -2.0, -2.5, -3.0, and -3.5. Corresponding values of *K* were calculated using equation (2). Thicknesses of ejecta (*T*) at the crater rim were then calculated using equation (1) with 340 m. Experimental data from explosion craters show that *s* varies from -1.97 to -3.65 (Roberts and Carlson, 1963) and can steepen to values of -6.5 near the crater rim (Carlson and Jones; 1965). Laboratory experiments with hypervelocity impact craters in sand (Stoffler and others, 1975, p. 4074) follow-equation (1) with an: average value of *s* of -3.3. McGetchin and others (1973) estimated that lunar craters probably obey equation (1) with *s* near: -3.0. The selected values of *s*, which cover the range of experimental data cited above, are given in table 1 with corresponding values

[1]Calculation of the thickness of material represented by fragment counts was performed as follows:

The fragments were assumed to have a spherical geometry, producing minimum volume estimates. (Cubic geometry would provide a maximum value, nearly double that calculated here) Fragment volumes were calculated using median diameters for each fragment-size range: 3.5 cm (2-5 cm), 7.5 cm (5-10 cm), 12.5 cm (10-15 cm), and 20 cm (greater than 15 cm). Percent areas covered by each size range were converted to an equivalent thickness by the formula:

$$\text{Thickness (m)} = \frac{\text{(fraction of area covered) (volume of fragments, m}^3\text{)}}{\text{(area covered by fragments, m}^2\text{)}}$$

Thicknesses derived from median diameters of fragment-size ranges are smaller than thicknesses calculated from median volumes of the same fragment-size end members (approximately 10 to 25 percent lower). The method used tends to compensate for the bias of fragment-size distributions toward the smaller size ranges.

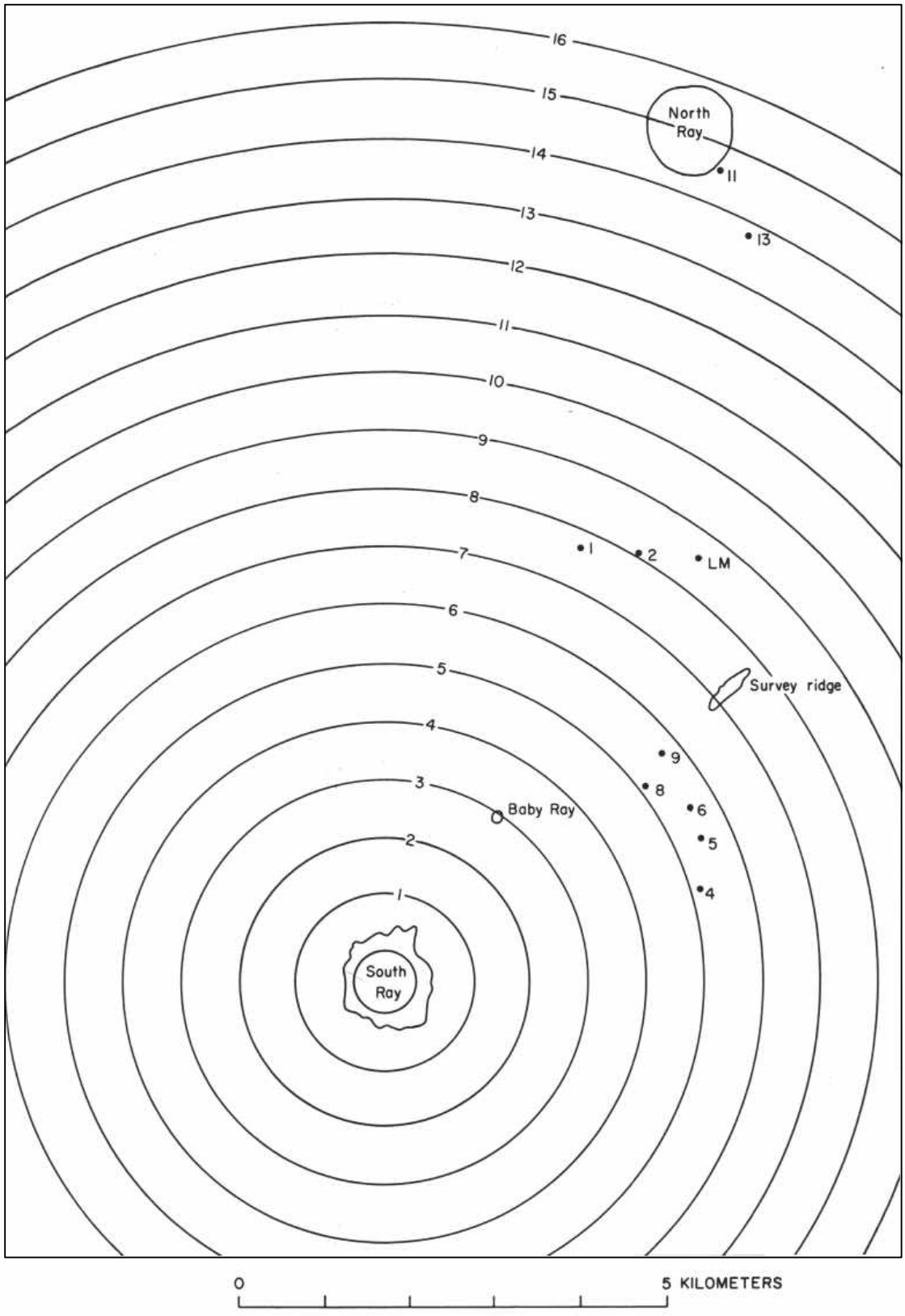

FIGURE 6.-Concentric rings centered on South Ray crater. The radius of each successive annulus is increased by one crater diameter. Area covered by ray material within each annulus was measured by planimeter at 1:50,000 scale. Station locations are shown by dots.

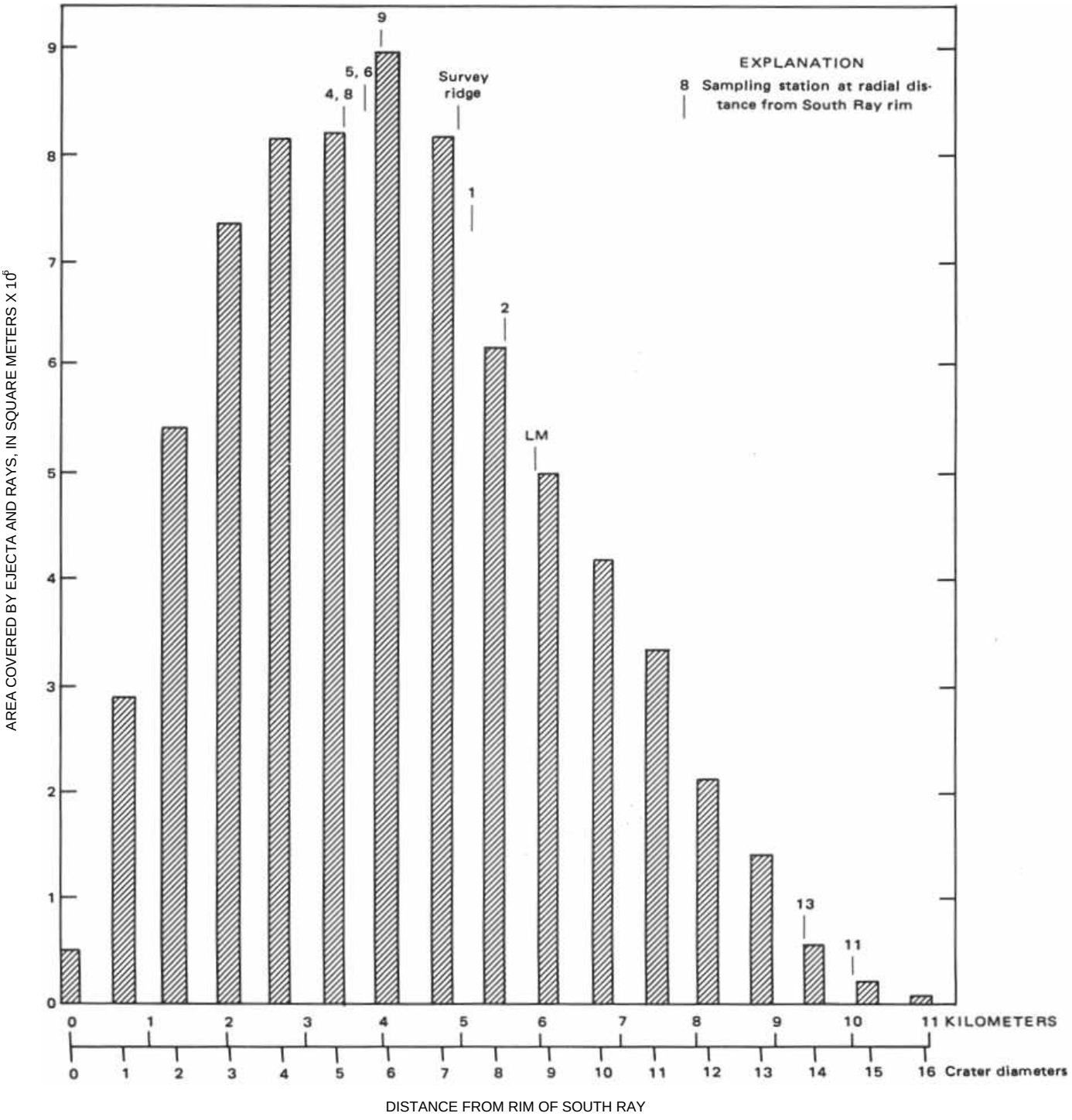

FIGURE 7.-Area covered by mappable ejecta and rays within each annulus shown in figure 6. Measurements are from superposed data of figures 3 and 6.

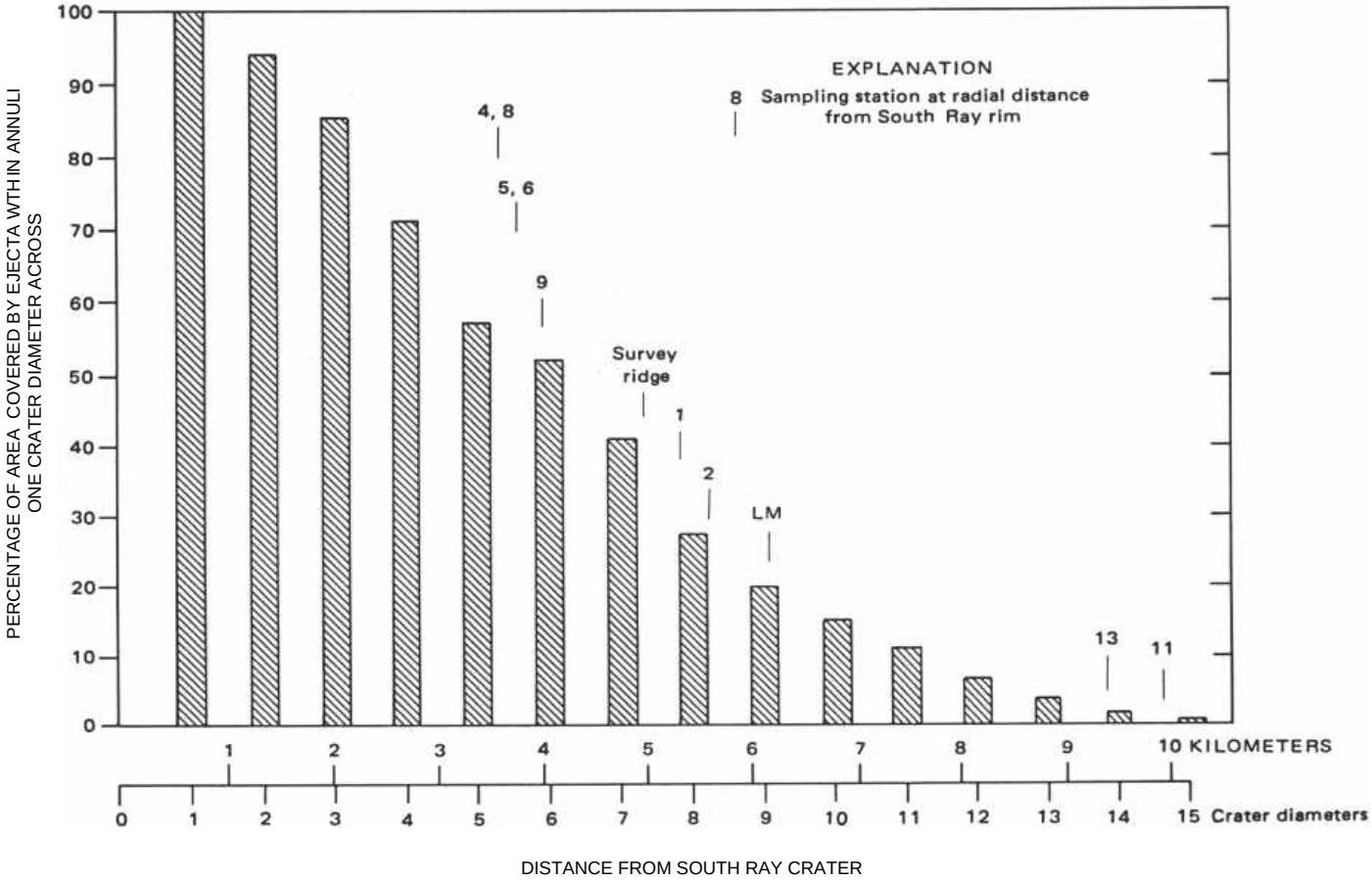

FIGURE 8.-Percentage of area covered by ejecta and rays in annuli of figure 6 relative to distance from South Ray crater rim.

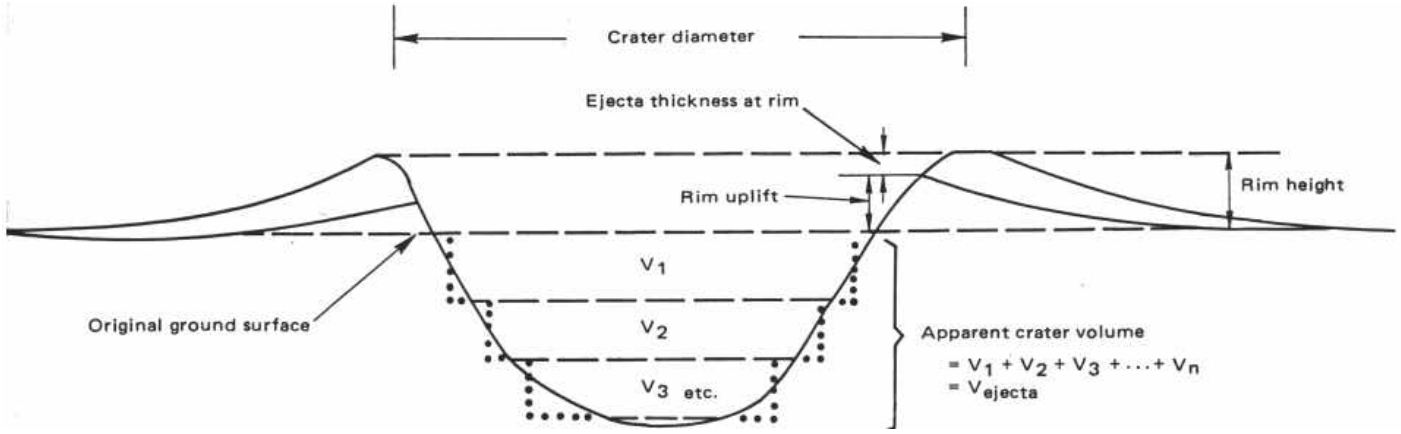

FIGURE 9.-Illustration of terms used for crater measurements discussed in text.

TABLE 1. -*Ejects distribution models for South Ray crater*
[Volume: l0x 10^6 m^3; crater radius: 340 m; rim height: 22 m]

Factors		Slope of ejecta thickness decay			
		-2	-2.5	-3	-3.5
Ejecta confined to mappable rays. Total volume deposited within 16 diameters	Constant, K……..	0.0688x10^7	2.15x10^7	60.8x10^7	1561x10^7
	Thickness at rim, *T* (meters)……..	5.9	10.1	15.5	21.5
	T/rim height…..……	0.27	0.46	0.70	0.98
	Fraction of volume beyond 16 diameters	0.0	0.0	0.0	0.0
Ejecta uniformly distributed at all azimuths to	Constant, K……..	[1].056x10^7	1.47x10^7	54.0x10^7	1497x10^7
	Thickness at rim, *T* (meters)……..	[2] 5.0	6.9	13.7	20.6
	T/rim height……..……	0.23	0.31	0.62	0.94
	Fraction of volume beyond 16 diameters	[3] 0	0.17	0.03	0.0053

[1]Calculated from equation using S=-2 and T=5 m.
[2]Assumed for calculation.
[3]No ejecta deposited beyond 16 diameters; volume of ejecta accounted for at 5,000 m from crater rim.

of *K* and *T* calculated from equations (2) and (1), respectively. The resulting thickness decay curves (fig. 11) can be compared with the calculated thicknesses of a uniform ejects deposit represented by fragments (larger than 2 cm) (shown in fig. 11 by-vertical. bars) representing the ranges of thickness determined from individual photographs. These data supersede those illustrated in an earlier paper. by Hodges and others (fig. 10, 1973), whose model assumed an ejects thickness of 10 m at the rim and predicted greater maximum thicknesses in the Apollo 16 traverse area than the present model by a factor of three to five from station 8 to station 13.

If the actual volume of ejects is 5 million m3 rather than the 10 million m3 measured above, model thicknesses. plotted in figure 11 and given in table 1 would be half the values indicated and the constant (*K*) would be half as large.

We can now evaluate the data and select a preferred ejects thickness distribution model for South Ray crater. The factors to be considered are slope (*s*), thickness at the rim (*T*), and *T*/rim height given in table 1: the resulting decay curves are plotted in figure 11, together with the ranges of thickness derived from fragment counts. If the fragments greater than 2 cm show an obvious relation to distance from South Ray crater, as they certainly do at Survey ridge (fig. 10*B*) and by their decrease away from South Ray (fig. 11), then there may be a contribution from fragments smaller than 2 cm. McKay and Heiken (1973, p. 45) argue from soil agglutinate contents, exposure ages, and size distribution of experimental crater ejects that relatively little fine-grained South Ray ejects (possibly 1 or 2 mm) would be expected in ray areas. Holt (this volume), however, maintains that the optical properties of the visible rays are likelier to be a product of fine-grained (comminuted) ejects than of coarse fragmental debris. It is possible that the dilution of fresh fines from South Ray due to mixing with old soils at the site may be so great that dating techniques cannot yet distinguish the younger materials.. The volume of fine material is probably not much greater than the volume of all fragments measured. Assuming an extreme case, that the fine-grained volume is twice the fragmental volume, the total thickness of ejects shown in figure 11 would increase approximately to the tops of the range bars shown for the fragments. The fragments counted may include a pre-South Ray population that in effect reduces the mean values attributable to the South Ray event.

The models for increasing values of *s* can be reviewed relative to the data of table 1 and the plot of figure 11. For s=-2, the value of *T* is 5.9 and 5.0 (assumed) for the confined and uniform models, respectively. These values result in thickness-to-rim-height ratios of 0.23 and 0.27; that is, 73 to 77 percent of the rim height is attributed to uplift, too high a percentage when compared with experimental data, though not an impossible value. In addition, both models: result in an excessive thickness (several millimeters) at the distance where the total volume is used up.

For s = -2.5, the decay curves for the confined model produce a reasonable *T*/rim-height ratio (0.46) because of the required thickness of ejects (10 m) at the rim. T is smaller (6:9 m) for the uniform model, wherein 17 percent of the total volume is still unused at 16 crater diameters. If the volume of fine-grained ejects (less than 2 cm) were more than twice that of the fragments counted. and if the fragments are assumed to have a cubic rather than spherical geometry, the decay curves for *s* = -2.5 produce a reasonable model. But because the total volume of 10 million m3 used in our calculations may be high by a factor of two, we believe that the preferred decay curve (fig. 11) must lie below that for *s* = -2.5.

For *s* = -3.0, the thickness-decay curves appear to be in fair agreement with the computed fragment volumes provided an additional volume of fines approximately equal to the fragment volume is allowed. This amounts to the equivalent of a few millimeters at station 8 and a few tenths of a millimeter at North Ray crater. The model gives *T*/rim-height ratios of 0.62 and 0.70 or 30-38 percent uplift, in reasonably good agreement with experimental data.

Finally, for *s* = -3.5, the values of *T* (20.6 and 21.5 m) and *T*/rim=height ratio (0.94 and 0.98) are too high relative to experimental data, and the corresponding thicknesses from figure 11 are too low relative to fragment counts. This model is therefore eliminated in favor of the model based on our measurements and calculations wherein *s* = -3.0.

It must be pointed out that the preferred model is only a best estimate at this time. The equations used

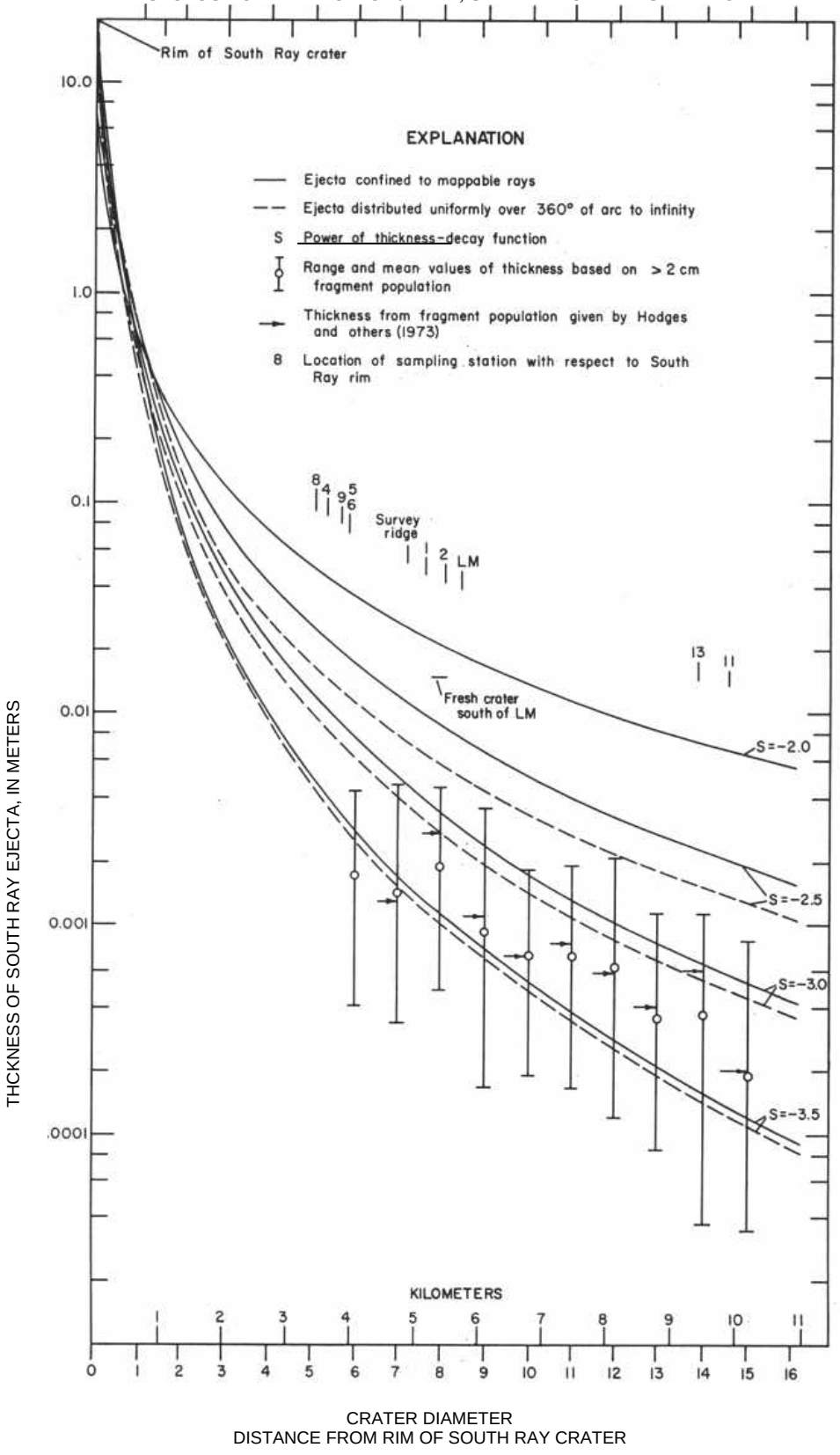

FIGURE 11.-Semilogarithmic plot showing thickness of ejects relative to distance from rim of South Ray crater. Curves are based on data from table 1 and calculations using equations 1 and 2 (see text) for total ejects volume of 10 million m^3.

there may not be an exact representation of the ejecta decay function. Other, more explicit functions may be required to describe in detail the thickness of ejecta as a function of distance from the crater; such refined data are not available at this. time.

SUMMARY

South Ray crater ejecta totaling about 10 million m3 covers the Apollo 16 landing site in an irregular radial pattern that reflects a nonuniform mantle of scattered debris. The ejecta thins rapidly from perhaps 10-15 m at the crater rim to 1 cm or less at the southern station localities (4, 5, 6, 8, and 9) and less than 1 mm at the northernmost stations (11 and 13). Using the general equation where thickness is a function of the crater radius to describe the thinning of ejecta with increasing distance from the crater, the preferred exponent for the radius is -3.0. The fragment population on the lunar surface (for sizes larger than 2 cm) accounts for a significant part of the total volume of ejecta. An ,equal amount of material finer than 2 cm can reasonably be accommodated by the preferred model.

Review of the photographic data, enhancement of the various levels of reflectance directly related to South Ray crater, and observations of evidence for ray materials on the surface provide a basis for assigning a South Ray origin to selected sample localities. With the information available at this time, we believe that station 8 has the highest potential for collection of South Ray fragments and fines; next highest are stations 9, 6, 4, and 5 in that order. The probability of collecting or identifying South Ray ejecta at stations farther away (>5 km from the crater) is considered very remote with the possible exception of station 2 samples, which may have been from the bright area at that locality. Determination of the provenance of individual samples will rely on additional evidence of other parameters-angularity, parchment, abundance of microcraters, particle-track ages, and rare-gas ages.

ACKNOWLEDGMENTS

This paper benefitted significantly from comments and suggestions of D. J. Roddy and W. R. Muehlberger. The work was done under NASA Contract T-5874A, except for that of H. J. Moore, done as part of NASA Experiment S-222.